JOURNAL OF MATERIALS SCIENCE 5 (1970) 295–301

Relationship Between Large Natural Strain and Resulting Hardness in AISI 1045 Steel Fractured under High Hydrostatic Pressures

D. R. McCANN, J. C. UY,* P. F. HETTWER
Allis Chalmers Manufacturing Company, Milwaukee, Wisconsin, USA

Environmental fluid pressures up to 184 ksi† were used during the tensile testing of AISI 1045 steel in order to achieve large ranges of strain beyond that normally obtainable at atmospheric pressure. Axial Knoop hardness measurements on the fractured specimens indicate that a power law relationship exists for this material between hardness, H, and natural strain, ϵ, in the form

$$H = H_0 \epsilon^n$$

where the exponent, n, is the strain-hardening index. It is also shown experimentally that this relationship is insensitive to the surrounding hydrostatic pressure at which the material is strained. On the basis of the above equation, the effect of billet hardness on the hydrostatic extrusion pressure is expressed theoretically.

1. Introduction

Since hydrostatic metal-forming is becoming an important process in the metalworking industry, it becomes desirable to achieve a better understanding of the behaviour of metals when worked under high hydrostatic pressures. Few data are available correlating hardness gradients produced in hydrostatically extruded products with stress-strain data [1]. Such a relationship is not only of interest in extrusion studies but is also useful for development of fabrication techniques in general.

Therefore, tensile straining under high pressure environments was conducted to determine whether a relationship could be obtained between flow stress, strain and resultant hardness.

2. Experimental Details

The material selected for investigation was AISI 1045 steel (0.45% C, 0.80% Mn, 0.03% P, 0.04% S, by weight). The tensile specimens (fig. 1) used for the *in situ* tests were machined from normalised 7.9 mm diameter cold-rolled rod. The normalisation process (815° C for 0.5 h) produced an average grain diameter of 1.5×10^{-2} mm.

The high pressure tensile apparatus is shown in fig. 2. The specimen was positioned in the chamber in such a way that the load platen was approximately 1.5 mm above the load cell. The pressure-transmitting medium was a 3:1 mixture of glycerine and ethylene glycol. The system was pressurised by application of a force $F1$ from a 75 ton‡ press. Care was taken to avoid loading the specimen during pressurisation by balancing the force $F2$ developed on the tension rod with a back force $F3$. At the desired chamber pressure, the back force $F3$ was reduced and regulated so that the tension rod advanced at a rate of approximately 0.5 mm min^{-1}. When the moving load platen contacted the rigid load cell, the specimen was placed in tension. The outputs of the load cell and of a linear potentiometer connected to the tension rod were fed into an X–Y recorder which produced a load-extension curve. The advancing tension rod was stopped when the desired strain was achieved, then the chamber pressure was reduced to atmospheric. The neck

*Presently at Battelle Memorial Institute, Metalworking Division, Columbus, Ohio, USA.
†1 ksi = 0.0689 k bar; ksi is the widely used abbreviation for, kilopounds per square inch, hydrostatic pressure.
‡1 ton = 1016 kg.

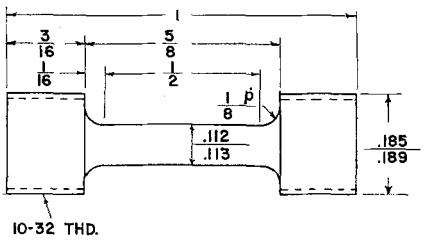

Figure 1 Tensile specimen. Units are in inches.

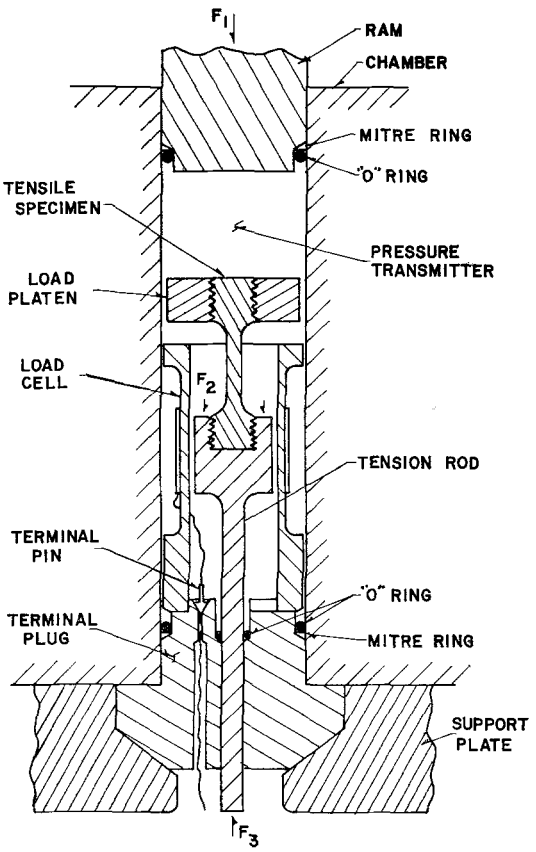

Figure 2 Tensile test apparatus.

diameter was measured and the radius of curvature of the specimen was determined photographically. This procedure was repeated approximately six times for each specimen until fracture occurred.

Longitudinal axial hardness data were obtained with a Knoop indenter using a 1 kg load. The specimen was mounted, ground and polished parallel to the axis, and then positioned in a fixture such that the surface was perpendicular to the indenter axis. Two series of hardness tests were made on each specimen with an intermittent repolishing between the two series of hardness measurements.

Fig. 3a shows the specimen grain structure far removed from the fracture tip, while fig. 3b shows the structure at the fracture tip. Because of the extreme amount of deformation which has occurred, it becomes difficult to speak of a grain size. For this reason, a comparison was not made between hardness and grain size [2].

3. Data and Discussion

3.1. Effect of Pressure on Yield and Tensile Strengths

Fig. 4 shows that the lower yield strength and tensile strength are not, within experimental error, affected by hydrostatic pressures up to 184 ksi.

3.2. Stress-Strain Relationship

The interrupted tensile data indicated that the relationship between the average true stress, σ, and natural strain, ϵ, can be represented, for these larger ranges of strain, by a parabolic equation

$$\sigma = \sigma_0 \epsilon^n$$

where σ_0 is a constant and n is the strain-hardening index. This relationship is common to many metals.

3.3. Strain-Hardening Indices

Experimentally, the strain-hardening index, n, can be determined in two ways. First, if the maximum load point on the load-extension curve is considered, it can be shown that the strain-hardening index can be expressed as

$$n = \log \left[\frac{A_0}{A_m}\right]$$

where A_0 = original cross-sectional area; A_m = cross-sectional area at maximum load point. Secondly, the index can be determined from the slope of an average true stress-natural strain curve on a log/log scale. However, Bridgman [3] pointed out that, in order to obtain the proper flow stress when determining the strain-hardening index, a correction should be applied to the average true stress. The correction results from localised necking which occurs during the tensile test. The corrected flow stress, F, is given by

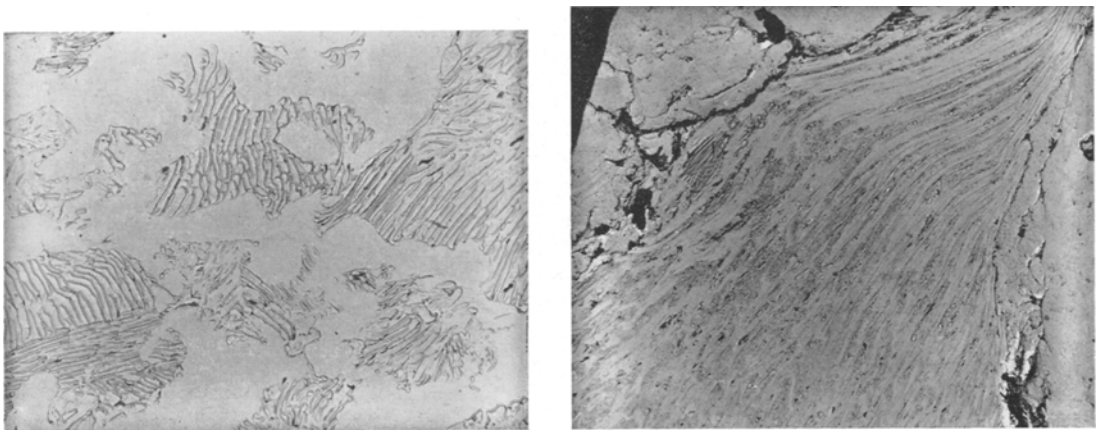

(a) (b)

Figure 3 Axial section through tensile specimen tested at 184 ksi showing deformation of microstructure. (a) Undeformed microstructure away from fracture tip. Plastic carbon replica (×1900). (b) Deformed microstructure at fracture tip. Plastic carbon replica (×1200).

F = average true stress × correction factor

or

$$F = \frac{L}{\pi r^2}\left[\frac{1}{\left(1 + \frac{2\rho}{r}\right)\log\left(1 + \frac{r}{2\rho}\right)}\right]$$

where L = load, r = neck radius, ρ = radius of curvature at neck. Figs. 5 and 6 show the corrected flow stress and average (uncorrected) true stress versus natural strain for different chamber pressures, respectively. The influence of the correction factor on lowering the slope of the line is quite obvious.

The indices from the methods discussed are tabulated in columns 2, 3, and 4 of table I. The deviation observed within each column is attributed to experimental error and slight difference in properties due to heat-treatment. There was no consistent nor significant change of the strain-hardening index with pressure. Therefore, it is believed that the strain-hardening index for this material is not sensitive to pressure;

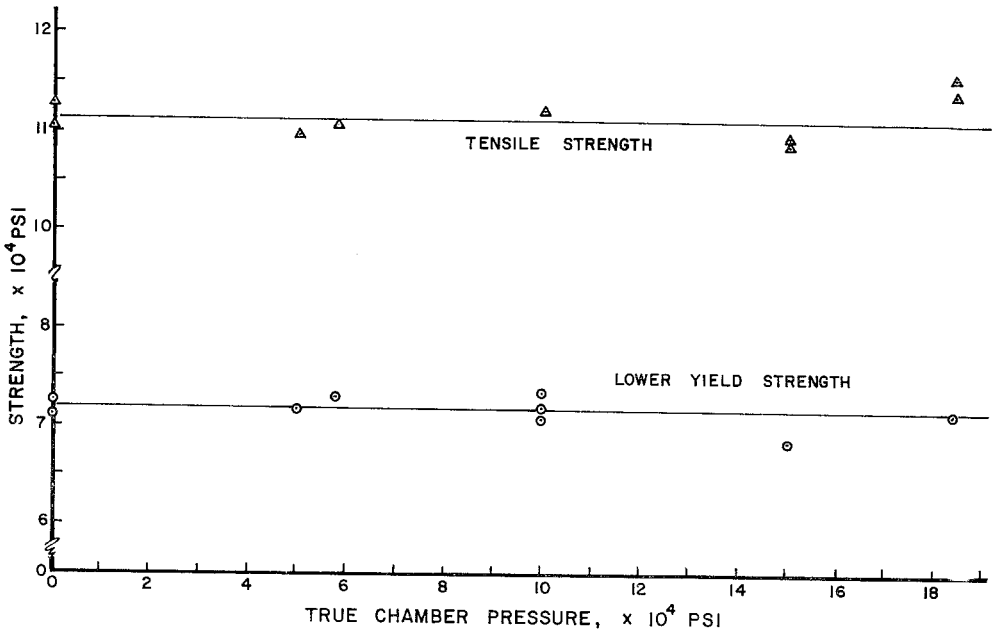

Figure 4 Effect of hydrostatic pressure on yield and tensile strengths.

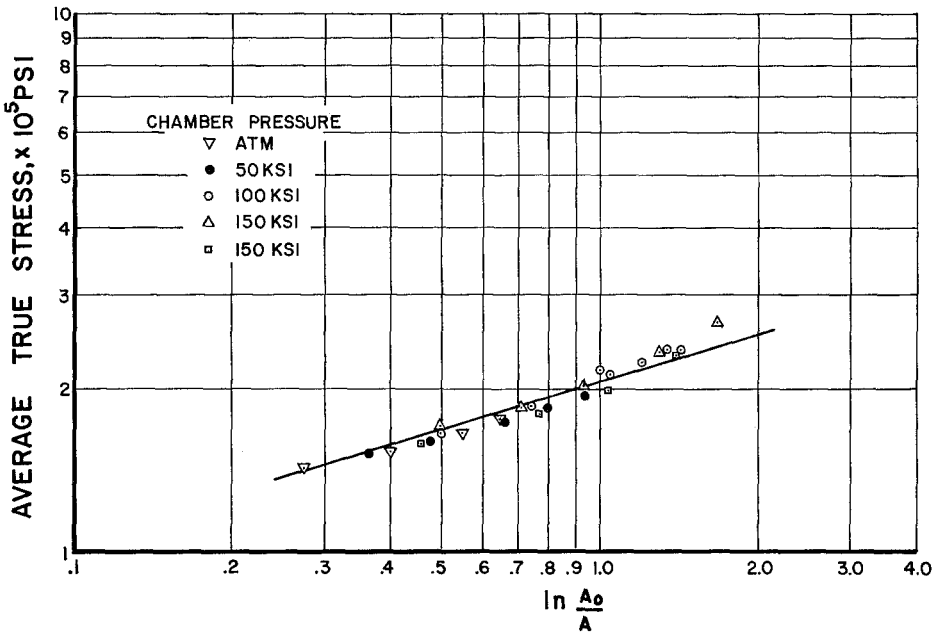

Figure 5 Flow stress versus natural strain.

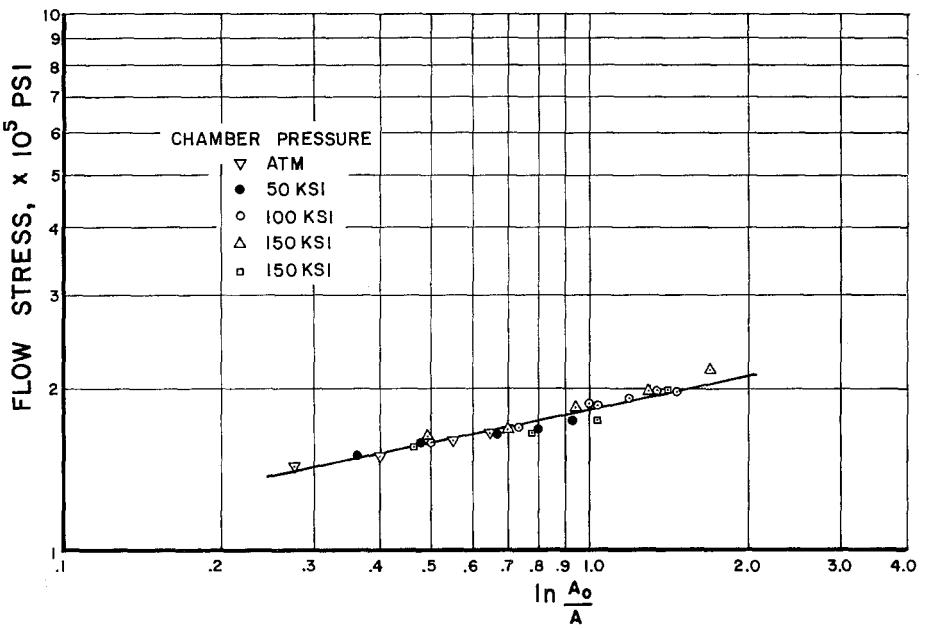

Figure 6 Average uncorrected true stress versus natural strain.

similar observations were made by Bridgman [3] and Pugh [1] on other metals. The maximum load and corrected flow stress indices are in good agreement with each other as shown by the overlap of their ranges and proximity of the average values. However, the uncorrected true stress index shows an appreciable deviation from the maximum load index and indicates that the stress must be corrected for necking effects.

3.4. Hardness-Strain Relationship

With the strain-hardening index thus established,

TABLE I Strain-hardening index

Chamber pressure (ksi)	Max.-load-point method	Uncorrected true stress method	Corrceted flow stress method	Knoop hardness method
Atmospheric	0.155	0.226	0.167	—
50 ksi	—	0.280	0.160	0.183
100 ksi	—	0.367	0.210	0.173
150 ksi	0.191	0.287	0.210	0.130
150 ksi	0.178	0.257	0.200	0.187
184 ksi	—	—	—	0.147
Range	0.155—0.191	0.226—0.367	0.160—0.210	0.130—0.187
Average	0.175	0.283	0.189	0.164

1 ksi = 0.0689 kbar.

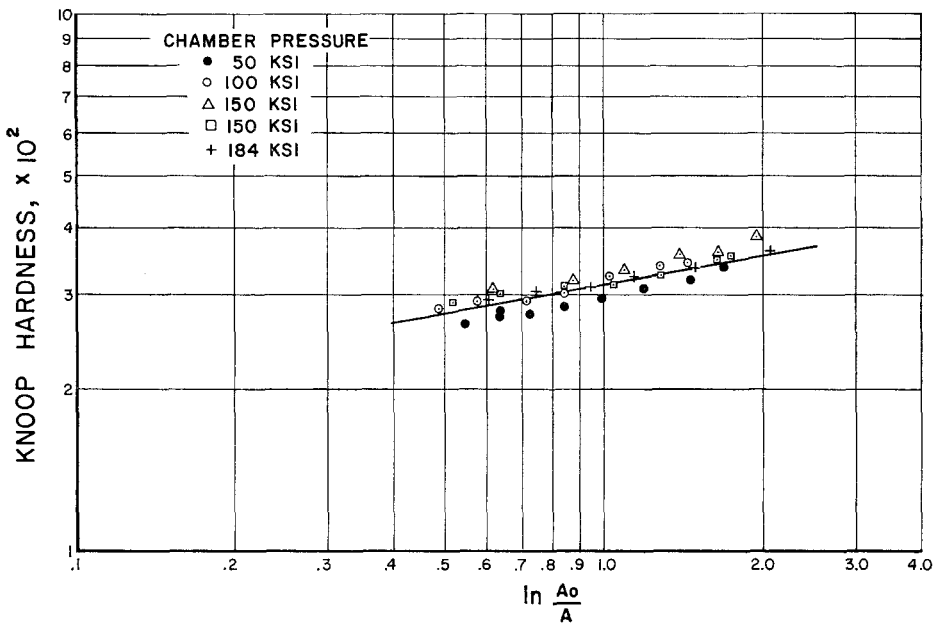

Figure 7 Axial hardness versus natural strain.

Knoop hardness measurements were made in the necked portion along the axis of the fractured tensile specimens. The major diagonal of the indenter was orientated perpendicularly to the specimen axis. The natural strain was computed at the region where each hardness measurement was taken. Fig. 7 shows axial hardness versus natural strain, and indicates that hardness and natural strain follow a power law relationship of the form

$$H = H_0\epsilon^n$$

where H_0 is a constant whose value is equal to the hardness of the material at $\epsilon = 1$. The n values determined by this method are tabulated in column 5, of table I. The exponents show a remarkable agreement with the strain-hardening index derived from the maximum load and flow stress methods, and also indicate that hardness is independent of hydrostatic pressure. Again, there appears to be no significance in the fluctuations among the results and these fluctuations are attributed to experimental error and slight variations of the initial hardness.

It is evident that the equation does not apply at very low strains because, as the strain approaches zero, so does the calculated hardness. This is contrary to actual conditions. The

initial hardness value of the steel, 220 Knoop, is equal to the extrapolated value obtained from fig. 7 at $\epsilon = 0.1$. Therefore, the equation is in error at strains of less than 0.1.

3.5. Hardness-Flow Stress Relationship

In the Knoop hardness test, the major diagonal of the indenter, which is the diagonal measured for computing the hardness, is seven times the minor diagonal and undergoes only a slight elastic recovery [4]. Thus, the unrecovered projected area can be computed. Since hardness is defined as load per unrecovered projected area, it should be related to some material stress level, which in this case appears to be the flow stress. If it is considered, on a first approximation basis, that the values of the strain-hardening index obtained from the hardness and stress methods are equal (as appears to be the case here) then the flow stress and hardness are directly related, that is,

$$\sigma = \left[\frac{\sigma_0}{H_0}\right] H .$$

The practical application implied by this relationship is that by measuring the hardness of a hydroformed component, and knowing σ_0 and H_0, an estimate of the localised flow stress can be obtained.

3.6. Hardness-Extrusion Pressure Relationship

A relationship can be obtained between the hydrostatic extrusion pressure and hardness. The extrusion pressure, P, is related to the hardness, H, by

$$P = \frac{\sigma_0 H_I}{(n+1)H_0}\left[\frac{2{\epsilon_1}^{n+1}}{(\log R)^n} + \log R + K(\log R)^2\right],$$

where R is the area extrusion ratio. This equation is derived in Appendix 1, and is in good agreement with an empirical expression found by Pugh [1]

$$P = 0.8\, H_I \log R$$

where P = extrusion pressure in 10^3 psi; H_I = diamond pyramid hardness. A sample calculation comparing both equations is shown in Appendix 2.

It should be noted that the derived equation may not apply to all materials because hardness is basically an empirical parameter which varies with type of test. It is not a fundamental material property.

4. Conclusion

The yield strength, tensile strength, and strain hardening index of AISI 1045 steel are invariant with environmental hydrostatic pressures up to 184 ksi. The axial Knoop hardness of strained tensile specimens can be related to the natural strain through a power law relationship. This same type of relationship also relates stress with strain and indicates one way that hardness can be related to flow stress. Therefore, by measuring the hardness of a hydroformed part, an estimate of the yield strength can be obtained. In addition, through the relationship of hardness and natural strain, the effect of hardness on the hydrostatic extrusion pressure has been shown.

Appendix 1

Relationship Between Extrusion Pressure and Initial Hardness

Pugh [5] states that the principal contributions to the total extrusion pressure include: (a) the minimum work per unit volume required to effect a homogeneous change in shape of the billet (homogeneous deformation, P_H); (b) the work done per unit volume in reversed shear at the entry and exit of the deformation zone of the die (redundant work, P_R); and (c) the work done per unit volume to overcome billet-die friction, P_F. The total extrusion pressure then becomes

$$P_T = P_H + P_R(\text{entry}) + P_R(\text{exit}) + P_F$$

or

$$P_T = \int_{\epsilon_1}^{\epsilon_2} \sigma d\epsilon + \int_{0}^{\epsilon_1} \sigma d\epsilon + \int_{\epsilon_2}^{\epsilon_3} \sigma d\epsilon + \frac{uR\log R}{(R-1)\sin\alpha}\int_{\epsilon_1}^{\epsilon_2} \sigma d\epsilon$$

where u = coefficient of coulomb friction, assumed < 0.1; R = area extrusion ratio; α = half-entrance cone angle of die; $\epsilon_1 = 0.5\,(\alpha/\sin^2\alpha - \cot\alpha)$; $\epsilon_2 = \epsilon_1 + \log R$; $\epsilon_3 = \epsilon_1 + \epsilon_2 = 2\epsilon_1 + \log R$.

Let $\sigma = \sigma_0\epsilon^n$ and $K = uR/(R-1)\sin\alpha$. Integrating and collecting terms

$$P_T = \frac{\sigma_0}{(n+1)}\left[{\epsilon_3}^{n+1} + K\log R\,({\epsilon_2}^{n+1} - {\epsilon_1}^{n+1})\right].$$

If n is small, then $(\epsilon_A + \epsilon_B)^{n+1} \approx {\epsilon_A}^{n+1} + {\epsilon_B}^{n+1}$

and

$$P_T = \frac{\sigma_0}{(n+1)}\left[2\epsilon_1{}^{n+1} + (\log R)^{n+1} + K\log R\,(\log R)^{n+1}\right]$$

$$= \frac{\sigma_0}{(n+1)}\left[2\epsilon_1{}^{n+1} + (\log R)\,(\log R)^n + K\,(\log R)^2\,(\log R)^n\right].$$

Substituting $\sigma_0 = \sigma/\epsilon^n = \sigma/(\log R)^n$ and $\sigma = \sigma_0/H_0\,H_I$

where H_I = initial hardness:

$$P_T = \frac{\sigma_0}{(n+1)}\frac{H_I}{H_0}\left[\frac{2\epsilon_1{}^{n+1}}{(\log R)^n} + \log R + K\,(\log R)^2\right].$$

Appendix 2

Comparison of Theoretical and Empirical Equations

The following conditions are assumed:

(a) The extrusion die angle is 45° or $\alpha = 22.5°$
(b) $R = 10$
(c) $\mu = 0.03$
(d) $H_I = 215$ Knoop hardness $= 200$ Diamond pyramid hardness
(e) $n = 0.175$
(f) $\sigma_0 = 185 \times 10^3$ psi,* obtained from fig. 5 at $\epsilon = 1$
(g) $H_0 = 310$ Knoop hardness $= 300$ Diamond pyramid hardness, obtained from fig. 7 at $\epsilon = 1$.

*1 psi = 0.0689 bar.

Substituting values $\epsilon_1 = 0.135$ and $K = 0.087$, then the theoretical extrusion pressure

$$P_T = \frac{\sigma_0}{(n+1)}\frac{H_I}{H_0}\left[\frac{2\epsilon_1{}^{n+1}}{(\log R)^n} + \log R + K\,(\log R)^2\right] = 3.6 \times 10^5 \text{ psi}$$

and, by Pugh's empirical equation [1], the extrusion pressure $P = 0.8\,H_I \log R = 3.7 \times 10^5$ psi. Thus the equations are in good agreement in this case.

Acknowledgement

This project was conducted under the supervision of Dr John Psarouthakis, Director of Technology, R&D Division The authors also wish to thank Mr Robert Vanark for his assistance in the experimental work, and Mrs Donna Meyer for her help in the preparation of the manuscript.

References

1. H. LL. D. PUGH, ASTM Special Technical Publication STP-374 (1964).
2. P. C. JINDAL and R. W. ARMSTRONG, *Trans Met. Soc. AIME* **239** (1967) 1857.
3. P. W. BRIDGMAN, "Studies in Large Plastic Flow and Fracture" (McGraw-Hill Book Co., New York, 1952).
4. S. R. WILLIAMS, "Hardness and Hardness Measurements" (American Society for Metals, Ohio, 1942).
5. H. LL. D. PUGH, *J. Mech. Eng. Sci.* **6** (1964) 362.

Received 12 August 1969 and accepted 6 January 1970.